NORHA, A Novel Follicular Atresia-related Lncrna, Promotes Granulosa Cell Apoptosis via miR-183-96-182 Cluster and FoxO1 Axis

Wang Yao
Nanjing Agricultural University - Weigang Campus: Nanjing Agricultural University
Zengxiang Pan
Nanjing Agricultural University College of Animal Science and Technology
Xing Du
Nanjing Agricultural University College of Animal Science and Technology
Jinbi Zhang
Nanjing Agricultural University College of Animal Science and Technology
Honglin Liu
Nanjing Agricultural University College of Animal Science and Technology
Qifa Li (liqifa@njau.edu.cn)
Nanjing Agricultural University College of Animal Science and Technology

Research Article

Keywords: follicular atresia, lncRNA NORHA, oxidative stress, granulosa cell apoptosis

Posted Date: March 22nd, 2021

DOI: https://doi.org/10.21203/rs.3.rs-331387/v1

Abstract

Background

Follicular atresia has been shown to be strongly associated with low follicle utilization rate and female infertility, which are regulated by many factors such as miroRNAs (miRNAs), a class of non-coding RNAs (ncRNAs). However, little is known about long non-coding RNAs (lncRNAs), another ncRNAs, which regulate follicular atresia.

Results

A total of 94 differentially expressed lncRNAs, including 74 up-regulated and 20 down-regulated lncRNAs, were identified in early atretic follicles compared to healthy follicles by RNA-sequencing. We identified and characterized a non-coding RNA that was highly expressed in atretic follicles (NORHA), an intergenic lncRNA, was the most significantly elevated lncRNA in early atretic follicles. Functionally, RT-PCR□flow cytometry and western blot results showed that NORHA was associated with follicular atresia by influencing GC apoptosis. Mechanistically, bioinformatics analysis, luciferase reporter assay and RNA immunoprecipitation assay results showed that NORHA acted as a 'sponge', which directly bound to the miR-183-96-182 cluster, and therefore resisted their targeting inhibition of FoxO1, the major sensor and effector of oxidative stress. Furthermore, NORHA and oxidative stress synergistically induced GC apoptosis.

Conclusions

We provide a comprehensive perspective of lncRNAs regulation of follicular atresia, and demonstrate that NORHA, a novel lncRNA related to follicular atresia, induces GC apoptosis through affecting the miR-183-96-182 cluster and Foxo1 axis

Introduction

The overall genome, non-coding RNAs (ncRNAs) such as microRNAs (miRNAs), ribosomal RNAs (rRNAs), transfer RNAs (tRNAs), long non-coding RNAs (lncRNAs), piwi-interacting RNAs (piRNAs), and circular RNAs (circRNAs), represent a larger part of the transcriptome than coding genes [1-3]. LncRNAs refer to a subclass of RNA polymerase II transcripts with a length of not less than 200 nucleotides (nt) and weak or non-coding potential [4, 5]. Compared with protein-coding genes and other ncRNAs, the lack of sequence conservation among species is a feature highlight of lncRNAs [6]. This confounded efforts to predict the sequences, functions, and mechanisms of action of lncRNAs across species [7]. For scientists, species-specific lncRNAs are like mysterious treasure, so using high-throughput technology to uncover species-specific lncRNAs is the focus of current research, and huge numbers of lncRNAs in various species have been identified [8]. Only a few lncRNAs have been functionally characterized, and as of 2018, only 156 lncRNAs had known biological functions [6, 9]. However, their functions are very extensive, and have been reported as essential regulators in various cell biological processes, such as cell survival [10],

differentiation [11], cell cycle [12], cell apoptosis [13], pluripotency [14], and susceptibility to infection [15]. In addition, unlike the relatively simple mechanism (RNA-RNA interaction) of action for miRNAs, the mechanism of function of lncRNAs is very diverse, and enables complex interactions with DNA, RNA, and proteins [9].

In the ovary, emerging data have demonstrated that lncRNAs are widely enriched in oocytes, various somatic cell types including granulosa cells (GCs), cumulus cells (CCs) and ovarian surface epithelial stem cells, and follicular fluid [16, 17]. These cells are associated with multiple ovarian functions, from maintenance and initiation of the primordial follicle pool to ovulation, corpus luteum formation, and ovarian aging [18-21]. Numerous lncRNAs were identified in somatic cells and oocytes at all stages of follicular development using high-throughput technology. For example, a total of 20,563 lncRNAs were identified in human CCs [22], and 4,926 differentially expressed lncRNAs (DELs) were identified in goat ovaries between the luteal and follicular phases [23]. However, only a few lncRNAs are well-characterized in terms of function and mechanism in humans and rodents [19, 24]. Nuclear enriched abundant transcript 1 (NEAT1), for instance, a lncRNA implicated in many major physiological events [25, 26]. NEAT1 is abundant in human metaphase II (MII) oocytes and mouse corpus luteum, and a Neat1 knockout (KO) mouse model revealed that luteal tissue formation was seriously diminished in nearly half of the Neat1 KO mice [16, 19]. Furthermore, ovarian lncRNAs have been shown to be related to livestock fecundity [27]and human infertility [28]. In addition, dysregulation and dysfunction of lncRNAs will result in ovarian diseases such as premature ovarian insufficiency (POI), polycystic ovary syndrome (PCOS), ovarian cysts, and cancer [24, 29].

In summary, there are many lncRNAs related to ovarian function identified by high-throughput methods [22, 23]; however, the function and molecular mechanism of only a small subset of lncRNAs are known. In this study, we performed RNA-seq to investigate lncRNA expression profiles in healthy follicles (HF) and early atretic follicles (EAF) of pig ovaries. Furthermore, we investigated the role and mechanism of NORHA, a lncRNA that was the most up-regulated in atretic follicles, to better understand the regulation of lncRNAs in follicular atresia.

Materials And Methods

Follicles collection and classification

Antral follicles with a diameter of 3–5 mm were procured from ovaries of mature sows, and then classified into HF and EAF group based on the ratio of progesterone (P4)/17β-estradiol (E2) concentration in follicular fluid, the GC density in follicular fluid, and the morphological features of follicles as previously described [30]. All animal experiments follow the ARRIVE guidelines and approved by the Ethical Committee of Nanjing Agriculture University.

RNA isolation and Sequencing

TRIzol reagent (Invitrogen, Shanghai, China) was used to isolate total RNA from follicles. The quality and integrity of total RNA were evaluated using an Agilent 2100 Bioanalyzer (California, USA) and agarose gel electrophoresis. The integrity score was no less than 7.0, and the ratio of 28S/18S of ribosomal RNA greater than 0.7 was set as the acceptable standard. After removing rRNA, total RNA of six healthy follicles or six early atretic follicles were constructed into one RNA-seq library. Paired-end sequencing was performed using an Illumina HiSeq2000.

Sequencing data analysis

The genome mapping of reads was performed by the TopHat v2.0.9 software (https://ccb.jhu.edu/software/tophat/index.shtml). The mapped reads were assembled by using a Cufflinks tool (http://cole-trapnell-lab.github.io/cufflinks/). Cuffcompare program (http://cole-trapnell-lab.github.io/cufflinks/cuffcompare/) was used to compare candidate sequences with known lncRNAs, and the differential expression analysis was performed by DESeq2 in the R package (https://www.r-project.org/). DELs was screen by the following criteria: (i) the length of transcripts ≥ 200 bp; (ii) the expression value with FRPKM > 0; (iii) the transcripts were predicted as a non-coding RNA in pig reference genome database (*Sus scrofa* 11.1); (iv) The screening criteria of DELs were established by a *P*-value ≤0.05 and a |logarithm to the fold-change in the expression of two| ≥ 0.5. Chromosomal locations, gene blast, annotated transcripts and sequence mapping were visualized on the genome data from NCBI database (https://www.ncbi.nlm.nih.gov/gene). Two online tools CPC (http://cpc.cbi.pku.edu.cn/) and CAPT (http://lilab.research.bcm.edu/cpat/index.php) were used to evaluate the coding potential of transcripts.

Functional enrichment analysis

To predict the potential functions of DELs, the *cis*-target mRNAs, which were selected within the range of 200 kb in the upstream and downstream of DELs, were annotated and classified by Gene ontology (GO) and Kyoto encyclopedia of genes and genome (KEGG) pathway analysis using DAVID Bioinformatics Resources v6.7 (https://david-d.ncifcrf.gov/).

Quantitative real-time RT-PCR

Total RNAs from tissues, follicles or GCs were extracted as described in RNA-sequencing, and the first-strand cDNA was synthesized from 500 ng of total RNA using the PrimeScript™ RT Master Mix (TaKaRa, Dalian, China). Differently, the reverse transcription of miRNAs was performed by TransScript miRNA First-Strand cDNA Synthesis SuperMix (TransGen, Beijing, China). RT-PCR was performed as described previously [31], and the primers are shown in Table S6.

Rapid amplification of cDNA ends

The 5'- and 3'-rapid amplification of cDNA ends (RACE) was performed to obtain the full-length of lncRNA. The first-strand cDNA was synthesized by using the SMARTer RACE cDNA Amplification Kit

(TaKaRa, Dalian, China). PCR was performed to amplify cDNA product from the 5’ end or 3’ end of NORHA with a gene-specific primers shown in Table S6.

Cell culture and treatment

GCs and HEK293T cells were cultured as described previously [31]. After the density reached 70–80%, cells were transfected by the Lipofectamine 3000 reagent (Invitrogen, Shanghai, China) following the manufacturer’s specifications. For H_2O_2 treatment, the medium was replaced with serum-free medium, different concentrate H_2O_2 (30 % [w/w] in H_2O, Sigma, Shanghai, China) were added to the medium for 90 min.

Plasmid construction

To construct the overexpression plasmid pcDNA3.1-NORHA, the full length of NORHA RNA was amplified from cDNA of porcine GCs by using a specific primer (Table S6) with *Hind*III and *Xho*I enzymes sites. The PCR product was digested with restriction enzymes and then inserted into the pcDNA3.1 vector (GenePharma, Shanghai, China) by T4 ligase for 24 h (Thermo Fisher, Waltham, MA, USA). Besides, The pcDNA3.1-FoxO1 vector was synthesized by YiDao (Nanjing, China). To identified the MRE of miR-183-96-182 cluster in NORHA or FoxO1 3’-UTR, the RNA fragment of FoxO1 3’-UTR or NORHA containing miRNA binding site was cloned into the pmirGLO Dual-Luciferase vector (Promega, Madison, WI, US). Meanwhile, MRE in FoxO1 3’-UTR or NORHA was mutated by using a Mut Express II Fast Mutagenesis Kit (Vazyme, Nanjing, China). Primers for plasmid construction are listed in Table S6.

Oligonucleotides

NORHA-specific or FoxO1-specific siRNAs, and mimics or inhibitor of miRNAs including miR-182, miR-96 and miR-183 listed in Table S7 were generated by GenePharma (Shanghai, China).

Apoptosis analysis

GCs apoptosis rate were measured by Apoptosis Detection Kit (Vazyme, Nanjing, China). Briefly, GCs were stained with 5 μl of Annexin FITC V and 5 μl of PI solution for 10 min, and the apoptosis rate was counted by BD FACScan flow cytometry (Becton Dickinson, Franklin, NJ, USA).

Western blotting

Western blotting were performed as described previously [31]. The primary antibodies used in study are anti-Caspase3 (CASP3) (diluted at 1:1000; Proteintech, Wuhan, China), anti-FoxO1 (diluted at 1:1000; CST, BMA, USA). Anti- Beta-Tubulin (diluted at 1:2000; Proteintech, Wuhan, China) was measured as an internal control.

Dual-luciferase reporter assay

Luciferase activities were detected by Luciferase Assay Buffer II and Stop & GLO Substrate with Modulus™ Assay System (Turner Biosystems, San Francisco, CA, USA) as described previously [31].

RNA immunoprecipitation (RIP) assay

RIP experiment was performed by using the EZ Magna RIP kit (Millipore, Billerica, MA, USA). The cells were pelleted and lysed in complete RIP lysis buffer containing protease inhibitor cocktail and RNase inhibitor. Homogenates were re-suspended to a single cell suspension and store at -80℃. Magnetic beads were washed several times with RIP wash buffer and then labelled with antibodies for 30 min. The extract was incubated with magnetic beads linking to AGO2 (CST, BMA, USA) or IgG antibodies (Santa Cruz, CA, USA) for overnight at 4 ˚C with head-to-head rotation. Finally, RT-PCR was performed to detect the expression of NORHA by specific primers shown in Table S6.

ROS detection

The ROS detection was performed by Reactive Oxygen Species Assay Kit (KeyGen, Shanghai, China). Briefly, GCs were incubated with DCFH-DA (diluted at 1:1000 in serum-free medium) for 20 min in 37 ℃, and the fluorescence of DCF in cells was detected by using BD FACScan flow cytometry (Becton Dickinson, Franklin, NJ, USA).

Statistical analysis

Statistical analysis was performed by using Graphpad Prism v5.0 software (San Diego, CA, USA). The level of significance was set to 0.05 and used the Student's t-test or one-way analysis of variance test. The correlation detection was analyzed using the Pearson test model. A P value of < 0.05 was considered to be associated, and the value of r represents the levels of correlation.

Results

Genome-wide identification of follicular atresia-related lncRNAs

To investigate the role of lncRNAs during follicular atresia, HF and EAF were isolated from porcine ovaries according to the P4/E2 ratio, the GC density, and the morphological features of follicles (Fig. 1a); and RNA-seq was used to construct the expression profiles of lncRNAs. A total of 10,066 transcripts and 1,918 lncRNAs were identified in follicles, 1,807 and 1,899 lncRNAs were detected in HF and EAF, and 1,574 lncRNAs were found in both HF and EAF (Fig. 1b, Table S1). The chromosomal distribution of follicular lncRNAs was not uniform, and the number of lncRNAs transcribed from chromosome 1 was the highest, while chromosome 10 was the lowest (Fig. 1c). Notably, a total of 94 DELs, including 74 up-regulated and 20 down-regulated lncRNAs, were identified in EAF compared to HF (Fig 1d, Table S2). To confirm the RNA-seq data, 7 DELs were selected for quantification by qRT-PCR. The data showed that the qRT-PCR of 6 DELs confirmed the accuracy of the RNA-seq data (Fig. 1e).

A total of 492 *cis*-target mRNAs of DELs were identified (Table S3), and GO analysis revealed that a total of 23 significant GO terms were enriched, for example, the positive regulation of apoptotic process, negative regulation of cell proliferation, sequence-specific DNA binding, and nucleoplasm (Fig. S1, Table S4). Besides, KEGG pathway analysis revealed that multiple significant pathways were enriched, such as the MAPK signaling pathway, oxytocin signaling pathway, DNA replication, and Insulin secretion (Fig. S2, Table S5).

NORHA was a novel cytoplasmic lncRNA involved in follicular atresia

Notably, in the first five DELs up-regulated during follicular atresia, qRT-PCR showed that LOC102167901 was the most significantly elevated DEL, which was selected for further analysis. We first isolated the full-length RNA sequence of porcine LOC102167901 from porcine ovaries by performing a RACE (Figs. 2a, and S3a). The full-length LOC102167901 novel transcript was 1,566 bp (Fig. S3b), which was different from the original sequences of LOC102167901 in the GenBank database (XR_304632, 7082 bp, predicted). The protein-coding ability scores of the LOC102167901-derived novel transcript were 0.067 (CPAT method) and -0.92330 (CPC method), which was close to that of other known lncRNAs (e.g., MALAT1 and H19) (Figure 2b, c), indicating that the novel transcript was devoid of protein-coding potential; it was a real lncRNA. We therefore termed this novel lncRNA as a non-coding RNA that was highly expressed in atretic follicles or NORHA.

NORHA is a sense lncRNA located in a region from 100135521 nt to 100137345 nt on the pig chromosome 7, and consists of two exons and one intron (Fig. 2a). The expression pattern revealed that NORHA was highest expression in ovary, but very weak in heart (Figs. 2d, and S4). The subcellular location showed that NORHA was enriched in the cytoplasm of porcine GCs (Fig. 2e). In ovarian follicles, NORHA levels were positively correlated with the P4/E2 ratio (r=0.3858, $P < 0.05$), a biomarker for follicular atresia, indicating that NORHA was involved in porcine follicular atresia (Fig. 2f). Taken together, we identified a novel cytoplasmic lncRNA, NORHA, in GCs and demonstrated that this lncRNA was involved in porcine follicular atresia.

NORHA induced GC apoptosis

In pigs and other mammals, follicular atresia has been shown to be triggered by GC apoptosis [31, 32]. To understand the relationship between NORHA and GC apoptosis *in vivo*, we examined the levels of NORHA and Caspase3, a pro-apoptotic marker for porcine GC apoptosis in follicles, and found that NORHA levels were positively correlated with Caspase3 mRNA levels (r=0.5845, $P < 0.01$) (Fig. 3a). To further determine the role of NORHA in porcine GC apoptosis, we overexpressed and silenced endogenous NORHA in GCs by treatment with pcDNA3.1-NORHA vector and NORHA-siRNA (Fig. 3b). Flow cytometry showed that NORHA overexpression increased the apoptosis rate of GCs (Fig. 3c), whereas silencing of NORHA decreased the apoptosis rate of GCs (Fig. 3d). In addition, cleaved Caspase3 (C-CASP3) protein levels were increased in GCs after overexpression of NORHA (Fig. 3e), whereas decreased in GCs after knockdown of NORHA (Fig. 3f). These results suggested that NORHA was a pro-apoptotic lncRNA in porcine GCs.

NORHA was a molecular sponge of the miR-183-96-182 cluster

The main mode of action of cytoplasmic lncRNA is to function as a “miRNA sponge” [33, 34]. To explore the molecular mechanism underlying cytoplasmic NORHA enhancement of porcine GC apoptosis, the co-expression network of NORHA and miRNAs (unpublished) during follicular atresia was constructed. The results suggested that NORHA potentially interacted with 21 miRNAs that were differentially expressed during follicular atresia (Fig. 4a). Interestingly, the miR-183-96-182 cluster, which are transcripts from a common genomic region (nt 18982506 – nt 18982590) on pig chromosome 18 (Figs. 4b, and S5), were predicted to bind to NORHA using RNAhybrid (Fig. 4c, d), indicating that the lncRNA NORHA was a putative molecular sponge of the miR-183-96a-182 cluster in sows.

To confirm whether NORHA bound to the miR-183-96-182 cluster, we generated a dual-luciferase reporter vector harboring the response element of the miR-183-96-182 cluster (Fig. 4e), and co-transfected it into HEK293T cells with miR-183, miR-96, or miR-182 mimics, respectively. Luciferase assays revealed that these miRNAs cluster significantly decreased the luciferase activity of the reporter vector (Fig. 4f). However, the three miRNAs had no effect on the luciferase activity of the reporter construct with a mutated binding site (Fig. 4g). These results suggested that NORHA could bind to the miR-183-96-182 cluster. RIP assay shown that the NORHA were enriched in AGO2, a member of RISC (RNA-induced silencing complex)(Fig. 4h), indicating that NORHA had the potential to bind to the miR-183-96-182 cluster. Furthermore, the miR-183-96-182 cluster was up-regulated in NORHA-silenced GCs (Fig. 4i). Together, our data suggested that NORHA directly interacted with, and could sponge, the miR-183-96-182 cluster in porcine GCs.

miR-183-96-182 cluster inhibited GC apoptosis

Our previous miRNA profile (unpublished) showed that the levels of three members of the miR-183-96-182 cluster were decreased in porcine EAF compared to HF (Fig. 5a). We then confirmed this using RT-PCR (Fig. 5b), indicating that this cluster participated in porcine follicular atresia. To evaluate the function of the miR-183-96-182 cluster on follicular atresia, miRNA mimics were used to exogenously overexpress the levels of these miRNAs in GCs. Overexpression of the miR-183-96-182 cluster obviously decreased the percentage of apoptotic cells (Fig. 5c), and markedly suppressed levels of C-CASP3 (Fig. 5e), indicating that the miR-183-96-182 cluster inhibited porcine GC apoptosis. In contrast, the percentage of apoptotic cells (Fig. 5d) and C-CASP3 levels (Fig. 5f) were significantly increased in the miR-183-96-182 cluster-silenced GCs. Our results suggested that the miR-183-96-182 cluster could impede GC apoptosis and follicular atresia in sows.

FoxO1 was a common target of the miR-183-96-182 cluster in GCs

To explore the mechanism of the miR-183-96-182 cluster prevention of GC apoptosis, we next identified their targets. A total of 148, 383, and 411 potential targets were predicted for miR-183, miR-96, and miR-182, respectively (Fig. S6a). Seventeen genes were commonly targeted by the miR-183-96-182 cluster (Fig. 6a). Of these, FoxO1, a core member of the forkhead box O (FoxO) family, which plays an extremely

important role in GC apoptosis in mammals [35, 36], was selected as a candidate target of the miR-183-96-182 cluster for further study. RNAhybrid showed that the FoxO1 3’-UTR of mammals, including pigs, not only had a high interaction capacity with the miR-183-96-182 cluster (Fig. 6b), but also contained a miRNA response element (MRE) of the miR-183-96-182 cluster at 2261 nt – 2267 nt (GenBank ID: NM_214014) (Figs. 6c, and S6b), indicating that FoxO1 was a potential target of the porcine miR-183-96-182 cluster.

To determine whether the miR-183-96-182 cluster directly targeted the porcine FoxO1 3’-UTR, we constructed a pmirGLO dual-luciferase reporter vector of the porcine FoxO1 3’-UTR containing the MRE motif (Figure S7a). HEK293T cells were transiently co-treated with this reporter plasmid and the miRNA mimics. The luciferase activity of the reporter vectors were significantly attenuated in cells treated with the miRNA mimics (Fig. 6d), but the luciferase activity of the MRE-mutated reporter vectors had no altered (Figs. 6e, and S7b), indicating that FoxO1 was a direct target of the miR-183-96-182 cluster in pigs. We next investigated whether the miR-183-96-182 cluster controlled FoxO1 expression in porcine GCs. As shown in Fig. 6f, g, the miR-183-96-182 cluster significantly restrained FoxO1 expression in GCs, at both the transcription and translation levels. Together, these results suggested that FoxO1 was a direct and functional target of the miR-183-96-182 cluster in porcine GCs.

NORHA induced FoxO1-mediated GC apoptosis by competing for the miR-183-96-182 cluster

To determine if NORHA, a ceRNA for the miR-183-96-182 cluster influence of FoxO1 transcription in porcine GCs, pcDNA3.1-NORHA and NORHA-siRNA were transfected into GCs. As shown in Fig. 7a, b manipulation of NORHA expression by the plasmid pcDNA3.1-NORHA significantly induced FoxO1 expression in GCs. Conversely, knockdown of NORHA by NORHA-specific siRNA significantly reduced FoxO1 expression in GCs (Fig. 7c, d), suggesting that NORHA was an epigenetic inducer of FoxO1 in porcine GCs. We next investigated whether NORHA enhanced FoxO1 expression by competing for the miR-183-96-182 cluster in porcine GCs. As expected, the miR-183-96-182 cluster could attenuate NORHA-induced FoxO1 expression in GCs (Fig. 7e).

NORHA, the miR-183-96-182 cluster, and FoxO1 are involved in GC apoptosis, which has been confirmed by the above results and other studies [35, 36]. We therefore investigated whether NORHA affected FoxO1-mediated cell apoptosis by competing for the miR-183-96-182 cluster in porcine GCs. Overexpression of FoxO1 induced GC apoptosis, whereas knockdown of FoxO1 reduced GC apoptosis, indicating that FoxO1 promoted porcine GC apoptosis (Fig. 7f), as observed in mice [35, 36]. Furthermore, we showed that FoxO1-induced GC apoptosis could be reversed by miRNA-182, and this process could also be inhibited by NORHA (Fig. 7g, h). These analyses suggested that NORHA induced FoxO1-mediated cell apoptosis by competing for the miR-183-96-182 cluster in porcine GCs.

NORHA and oxidative stress synergistically induced GC apoptosis

FoxO1 is widely regarded as a major sensor and effector of oxidative stress; oxidative stress is a strong inducer of GC apoptosis in mammals [35, 37]. We therefore hypothesized that NORHA were involved in

oxidative stress-induced GC apoptosis. To validate this hypothesis, we first investigated the effects of oxidative stress driven by H_2O_2 treatment on porcine GC apoptosis. As shown in Fig. 8a, H_2O_2 can induce an increase in ROS levels in GCs. Meanwhile, the cell apoptosis rate and C-CASP3 levels were up-regulated in GCs with continuing H_2O_2 stimulation (Fig. 8b, c), indicating that short-term oxidative stress driven by H_2O_2 treatment promoted porcine GC apoptosis. Furthermore, overexpression of NORHA induced the apoptosis rate in GCs with H_2O_2 exposure (Fig. 8d), revealing that NORHA and oxidative stress could synergistically induce GC apoptosis.

Discussion

A large number of primordial follicles exist in the ovarian follicle pool in mammals; approximately 420,000 in pigs and 400,000 in humans. However, less than 1% of follicles mature and ovulate, while most follicles are atretic and degenerate [38]. Therefore, follicular atresia not only restricts the effective utilization of the primordial follicle pool, but also limits the potential reproductive ability of domestic animals. Many factors (e.g., follicle-stimulating hormone (FSH), Liver receptor homolog-1 (LRH-1), and X-linked inhibitor of apoptosis (XIAP)) and signaling pathways (e.g., death receptor-mediated, follicle stimulating hormone receptor (FSHR), and TGF-β signaling pathways) related to follicular atresia have been identified [31, 35, 39-42]. In recent years, high-throughput technology has gradually become an important way to fully understand the molecular events during follicular atresia, and the expression profile of miRNAs [30] and mRNAs [43] in follicular atresia has been revealed. Here, we profiled lncRNA expression patterns during follicular atresia using high-throughput RNA-seq, and 94 DELs were identified. Regulation of adjacent or host genes via *cis* regulation is a main functional model of lncRNAs [44, 45]. Notably, among the *cis*-target mRNAs of these DELs, multiple genes, such as CYP11A1 [46], BABAM2 [47], fibroblast growth factor 18 (FGF18) [48], and neurogenic locus notch homolog protein 2 (NOTCH2) [49] have been implicated in GC functions (e.g., steroid hormone synthesis), follicular atresia, ovarian functions, and female fertility. Our findings are the first to identify lncRNAs during follicular atresia and provide an understanding of lncRNAs that are involved in follicular atresia.

We further demonstrated that NORHA, the most up-regulated lncRNA during porcine follicular atresia, was strongly involved in porcine follicular atresia, through enhancing GC apoptosis. In GCs, lncRNAs have been reported to be associated with various cellular functions, such as proliferation and cycle [24, 28], and the secretion of steroid hormones, including E2, P4, and testosterone (T) [50, 51]. However, few studies have investigated the regulation of GC apoptosis by lncRNAs. A recent study showed that lncRNA steroid receptor RNA activator (SRA), an important player in transcriptional regulation, is thought to interact with a DNA-binding protein by binding to specific DNA sequences [52], which induces the release of E2 and P4, and reduces cell apoptosis in mouse GCs [51]. The Prader–Willi region non-protein coding RNA 2 (PWRN2), a CCs-expressed lncRNA, is thought to be associated with oocyte nuclear maturation through sponging miR-92b-3p in the human ovary [53]. In addition, in ovarian cancer cells, some lncRNAshave also been demonstrated to be involved in various cellular processes [29]. MLK7-AS1, for instance, an lncRNA that is specifically upregulated in ovarian cancer tissues, which controls multiple

cellular processes (e.g., it stifles cell invasion, proliferation, wound healing, and advances cell apoptosis), modulates the epithelial-mesenchymal transition (EMT) process by influencing the miR-375/Yes-associated protein 1 (YAP1) axis [29]. Taken together, our findings are the first to identify and characterize lncRNAs associated with follicular atresia, and provide evidence that NORHA could serve as a potential diagnostic biomarker and rescue target for follicular atresia.

As an important regulatory RNA, lncRNAs exert their biological function mainly by regulating target expression at various levels, from transcription to protein localization, and stability [9]. The subcellular localization (cytoplasm and/or nucleus) of lncRNAs is the principal determinant of their molecular function and mode of action [54]. The most common mechanism of action of both cytoplasmic and nuclear lncRNAs is to function as a ceRNA, regulating target gene expression via an lncRNA-miRNA-target model [9, 33, 54]. For instance, lncRNA-protein phosphatase 1 nuclear-targeting subunit (PNUTS), a non-coding isoform of the protein-coding gene PNUTS, serves as a ceRNA of miR-205 to influence the EMT migration and invasion by controlling the miR-205/ZEB/E-cadherin axis [55]. More recently, temozolomide -associated lncRNA (TALC), a highly expressed lncRNA in temozolomide-resistant glioblastoma, has been demonstrated to function as a ceRNA to competitively bind miR-20b-3p to enhance c-Met expression [33]. TALC then activates the Stat3/p300 complex to increase the transcriptional activity of the O^6-methylguanine-DNA methyltransferase by modulating the acetylation of H3, including H3K9, H3K27, and H3K36 [33]. Here, based on the NORHA-miRNA interactive network, we detected a putative binding site of the miR-183-96-182 cluster in NORHA, and demonstrated that NORHA functioned as a ceRNA for the miR-183-96-182 cluster, relieving its inhibition of the target FoxO1 and promoting cell apoptosis in porcine GCs.

The miR-183-96-182 cluster (or miR-183 cluster) is a polycistronic miRNA cluster, which is located within a 5-Kb genomic region on chromosome 7 in humans, chromosomes 6 in mice, and chromosome 18 in pigs. Importantly, this family is not only highly conserved among different species, but also has similar seed sequences among different members of the same species, implying that the members of this cluster may share the same targets and biological functions [56, 57]. Consistent with this hypothesis, recent reports showed that the miR-183-96-182 cluster common targets are HDAC9, which encodes a histone deacetylase that influences memory formation [58], Cacna2d2, which encodes the auxiliary voltage-gated calcium channel subunits α2δs to scale mechanical pain sensitivity [56], and DAP12 and Nox2, to control macrophage functions in response to *Pseudomonas aeruginosa* [59]. In addition, increased the miR-183-96-182 cluster in luteal relative to follicular tissues could enhance cell survival and P4 release in ovarian luteal cells of both bovine and humans by targeting bovine and human FoxO1, respectively [60]. Herein, we demonstrated that the miR-183-96-182 cluster was down-regulated in atretic follicles, inhibited the common target FoxO1 gene and mediated NORHA regulation of cell apoptosis in porcine GCs. In the ovary, the miR-183-96-182 cluster was mainly expressed in both follicular GCs and the corpus luteum, which plays a vital role in cell proliferation and the cell cycle of bovine GCs [61]. Together, our work indicated that the miR-183-96-182 cluster was related to follicular atresia by repression of GC apoptosis.

Determination of the mechanism of the miR-183-96-182 cluster repression of GC apoptosis led us to identify FoxO1 as a functional target of the miR-183-96-182 cluster, which mediated the anti-apoptotic function of the miR-183-96-182 cluster in GCs. FoxO1, a member of the FOXO family, has been shown to be a direct target of dozens of miRNAs, including the miR-183-96-182 cluster in mammals [35, 57]. As a functional target of the miR-183-96-182 cluster, FoxO1 participated in the miR-183-96-182 cluster regulation of multiple functions in various cells and tissues, such as cell death in endometrial cancer [62], pathogenicity in Th17 cells [57], adipogenesis in C2C12 myoblasts [63], and sperm quality in mouse testes [64]. Notably, in ovarian GCs, FoxO1 also mediates the miR-183-96-182 cluster regulation of GC functions [61]. In bovine GCs, for instance, FoxO1 is inhibited by the miR-183-96-182 cluster and can abate the proportion of cells in the S phase [61]. In addition, FoxO1 is thought to be associated with other GC functions, such as autophagy [34], apoptosis [35], proliferation [61] and differentiation [65], and response to FSH [66].

Conclusion

Collectively, our work detected alterations in lncRNA expression in health and early atretic follicles, and identified a novel lncRNA, NORHA, which was highly expressed in atretic follicles. NORHA induced follicular atresia and GC apoptosis via a miR-183-96-182 cluster/FoxO1 axis by competitively sponging the miR-183-96-182 cluster (Fig. S8). Our findings uncovered new epigenetic mechanisms of follicular atresia and GC apoptosis, providing evidence that NORHA could serve as a potential diagnostic biomarker and rescue target for follicular atresia, as well as a novel candidate for the improvement of female fertility.

Abbreviations

ncRNA: long noncoding RNA;

NORHA: non-coding RNA that was highly expressed in atretic follicles;

FoxO1: forkhead box O1;

TGF-β: transforming growth factor-β;

SMAD4: sma-and mad-related protein 4;

NEAT1: Nuclear enriched abundant transcript 1;

PCOS: polycystic ovary syndrome;

POI: premature ovarian insufficiency ;

P4: Progesterone;

E2: 17β-estradiol;

HF: Healthy follicles;

EAF: Early atretic follicles ;

GO: Gene ontology; KEGG:

Kyoto encyclopedia of genes and genome;

T-CASP3: Total Caspase-3;

C-CASP3: Cleave Caspase-3;

CPAT: coding-potential assessment tool;

CPC: coding potential calculator;

ROS: Reactive Oxygen Species;

FSH: follicle-stimulating hormone;

LRH-1: Liver receptor homolog-1;

XIAP: X-linked inhibitor of apoptosis;

FSHR: follicle stimulating hormone receptor;

BMP: bone morphogenetic protein;

YAP1: Yes-associated protein 1;

NOTCH2: neurogenic locus notch homolog protein 2

PNUTS: protein phosphatase 1 nuclear-targeting subunit;

TALC: temozolomide-associated lncRNA;

TMZ: temozolomide;

STAT5: Signal transducer and activator of transcription 5;

FOXP3: forkhead box P3;

MFE: Minimum Free Energy;

FACS: Fluorescence activated Cell Sorting;

MRE: miRNA response element

Declarations

Authors' contributions

Wang Yao, Honglin Liu, Qifa Li designed the idea; Wang Yao, Xing Du and Jinbi Zhang performed the experiments; Wang Yao and Zengxiang Pan analyzed the data; Qifa Li wrote the manuscript; Jinbi Zhang revised the manuscript. All authors have read and approved the final manuscript.

Declarations

Not applicable.

Funding

This work was supported by the National Natural Science Foundation of China (32072693 and 31630072) and the Qing Lan Project of Jiangsu Province (2020).

Competing interests

The authors declare that they have no competing interests.

Ethics approval and consent to participate

All animal experiments follow the ARRIVE guidelines and approved by the Ethical Committee of Nanjing Agriculture University.

Consent for publication

Not applicable

Acknowledgements

Not applicable

Availability of data and materials

Not applicable.

References

1. Gomes CPC, Schroen B, Kuster GM, Robinson EL, Ford K, Squire IB, Heymans S, Martelli F, Emanueli C, Devaux Y. Regulatory RNAs in heart failure. Circulation. 2020;141:313-328.

2. Nair L, Chung H, Basu U. Regulation of long non-coding RNAs and genome dynamics by the RNA surveillance machinery. Nat Rev Mol Cell Biol. 2020;21:123-136.
3. Anastasiadou E, Jacob LS, Slack FJ. Non-coding RNA networks in cancer. Nat Rev Cancer. 2018; 18:5-18.
4. Ponnusamy M, Liu F, Zhang YH, Li RB, Zhai M, Liu F, et al. Long Noncoding RNA CPR (Cardiomyocyte Proliferation Regulator) Regulates Cardiomyocyte Proliferation and Cardiac Repair. Circulation. 2019;139:2668-2684.
5. Papaioannou D, Petri A, Dovey OM, Terreri S, Wang E, Collins FA, et al. The long non-coding RNA HOXB-AS3 regulates ribosomal RNA transcription in NPM1-mutated acute myeloid leukemia. Nat Commun. 2019;10:5351.
6. Ransohoff JD, Wei Y, Khavari PA. The functions and unique features of long intergenic non-coding RNA. Nat Rev Mol Cell Biol. 2018;19:143-157.
7. Quinn JJ, Chang HY. Unique features of long non-coding RNA biogenesis and function. Nat Rev Genet. 2016;17:47-62.
8. Uszczynska-Ratajczak B, Lagarde J, Frankish A, Guigó R, Johnson R. Towards a complete map of the human long non-coding RNA transcriptome. Nat Rev Genet. 2018;19:535-548.
9. Flippot R, Beinse G, Boilève A, Vibert J, Malouf GG. Long non-coding RNAs in genitourinary malignancies: a whole new world. Nat Rev Urol. 2019;16:484-504.
10. Kotzin JJ, Iseka F, Wright J, Basavappa MG, Clark ML, Ali MA, et al. The long noncoding RNA Morrbid regulates CD8 T cells in response to viral infection. Proc Natl Acad Sci U S A. 2019; 116:11916-11925.
11. Luo J, Wang K, Yeh S, Sun Y, Liang L, Xiao Y, et al. LncRNA-p21 alters the antiandrogen enzalutamide-induced prostate cancer neuroendocrine differentiation via modulating the EZH2/STAT3 signaling. Nat Commun. 2019;10:2571.
12. Arab K, Karaulanov E, Musheev M, Trnka P, Schäfer A, Grummt I, et al. GADD45A binds R-loops and recruits TET1 to CpG island promoters. Nat Genet. 2019;51:217-223.
13. Chen F, Chen J, Yang L, Liu J, Zhang X, Zhang Y, et al. Extracellular vesicle-packaged HIF-1alpha-stabilizing lncRNA from tumour-associated macrophages regulates aerobic glycolysis of breast cancer cells. Nat Cell Biol. 2019;21:498-510
14. Ye B, Liu B, Yang L, Zhu X, Zhang D, Wu W, et al. LncKdm2b controls self-renewal of embryonic stem cells via activating expression of transcription factor Zbtb3. EMBO J. 2018;37 (8):e97174.
15. Kulkarni S, Lied A, Kulkarni V, Rucevic M, Martin MP, Walker-Sperling V, et al. CCR5AS lncRNA variation differentially regulates CCR5, influencing HIV disease outcome. Nat Immunol. 2019; 20(7): 824-834.
16. Bouckenheimer J, Fauque P, Lecellier CH, Bruno C, Commes T, Lemaître JM, et al. Differential long non-coding RNA expression profiles in human oocytes and cumulus cells. Sci Rep. 2018;8:2202.

17. Jiao J, Shi B, Wang T, Fang Y, Cao T, Zhou Y, et al. Characterization of long non-coding RNA and messenger RNA profiles in follicular fluid from mature and immature ovarian follicles of healthy women and women with polycystic ovary syndrome. Hum Reprod. 2018;33:1735-1748.
18. Zheng L, Luo R, Su T, Hu L, Gao F, Zhang X. Differentially Expressed lncRNAs After the Activation of Primordial Follicles in Mouse. Reprod Sci. 2019;26:1094-1104.
19. Nakagawa S, Shimada M, Yanaka K, Mito M, Arai T, Takahashi E, et al. The lncRNA Neat1 is required for corpus luteum formation and the establishment of pregnancy in a subpopulation of mice. Development. 2014;141:4618-27.
20. Yerushalmi GM, Salmon-Divon M, Yung Y, Maman E, Kedem A, Ophir L, Elemento O, Coticchio G, Dal Canto M & Mignini Renzinu M et al. (2014) Characterization of the human cumulus cell transcriptome during final follicular maturation and ovulation. Mol Hum Reprod 20, 719-35.
21. Cuomo D, Porreca I, Ceccarelli M, Threadgill DW, Barrington WT, Petriella A, et al. Transcriptional landscape of mouse-aged ovaries reveals a unique set of non-coding RNAs associated with physiological and environmental ovarian dysfunctions. Cell Death Discov. 2018;4:112.
22. Xu XF, Li J, Cao YX, Chen DW, Zhang ZG, He XJ, et al. Differential Expression of Long Noncoding RNAs in Human Cumulus Cells Related to Embryo Developmental Potential: A Microarray Analysis. Reprod Sci. 2015;22:672-8.
23. Liu Y, Qi B, Xie J, Wu X, Ling Y, Cao X, et al. Filtered reproductive long non-coding RNAs by genome-wide analyses of goat ovary at different estrus periods. BMC Genomics. 2018;19:866.
24. Zhao J, Xu J, Wang W, Zhao H, Liu H, Liu X, et al. Long non-coding RNA LINC-01572:28 inhibits granulosa cell growth via a decrease in p27 (Kip1) degradation in patients with polycystic ovary syndrome. EBioMedicine.2018;36:526-538.
25. Wang Y, Hu SB, Wang MR, Yao RW, Wu D, Yang L, et al. Genome-wide screening of NEAT1 regulators reveals cross-regulation between paraspeckles and mitochondria. Nat Cell Biol. 2018;20:1145-1158.
26. Zhang P, Cao L, Zhou R, Yang X, Wu M. The lncRNA Neat1 promotes activation of inflammasomes in macrophages. Nat Commun. 2019;10:1495.
27. Miao X, Luo Q, Zhao H, Qin X. Co-expression analysis and identification of fecundity-related long non-coding RNAs in sheep ovaries. Sci Rep. 2016;6:39398.
28. Liu YD, Li Y, Feng SX, Ye DS, Chen X, Zhou XY, et al. Long Noncoding RNAs: Potential Regulators Involved in the Pathogenesis of Polycystic Ovary Syndrome. Endocrinology. 2017;158:3890-3899.
29. Yan H, Li H, Li P, Li X, Lin J, Zhu L, et al. Long noncoding RNA MLK7-AS1 promotes ovarian cancer cells progression by modulating miR-375/YAP1 axis. J Exp Clin Cancer Res. 2018;37:237.
30. Lin F, Li R, Pan ZX, Zhou B, Yu DB, Wang XG, et al. miR-26b promotes granulosa cell apoptosis by targeting ATM during follicular atresia in porcine ovary. PLoS One. 2012;7:e38640.
31. Du X, Zhang L, Li X, Pan Z, Liu H, Li Q. TGF-beta signaling controls FSHR signaling-reduced ovarian granulosa cell apoptosis through the SMAD4/miR-143 axis. Cell Death Dis. 2016;7: e2476.

32. Matsuda F, Inoue N, Manabe N, Ohkura S. Follicular growth and atresia in mammalian ovaries: regulation by survival and death of granulosa cells. J Reprod Dev. 2012;58:44-50.
33. Fatica A, Bozzoni I. Long non-coding RNAs: new players in cell differentiation and development. Nat Rev Genet. 2014;15:7-21.
34. Wu P, Cai J, Chen Q, Han B, Meng X, Li Y, et al. Lnc-TALC promotes O(6)-methylguanine-DNA methyltransferase expression via regulating the c-Met pathway by competitively binding with miR-20b-3p. Nat Commun. 2019;10:2045.
35. Shen M, Jiang Y, Guan Z, Cao Y, Li L, Liu H, et al. Protective mechanism of FSH against oxidative damage in mouse ovarian granulosa cells by repressing autophagy. Autophagy. 2017;13:1364-1385.
36. Zhang M, Zhang Q, Hu Y, Xu L, Jiang Y, Zhang C, et al. miR-181a increases FoxO1 acetylation and promotes granulosa cell apoptosis via SIRT1 downregulation. Cell Death Dis. 2017;8:e3088.
37. Sewastianik T, Szydlowski M, Jablonska E, Bialopiotrowicz E, Kiliszek P, Gorniak P, et al. FOXO1 is a TXN- and p300-dependent sensor and effector of oxidative stress in diffuse large B-cell lymphomas characterized by increased oxidative metabolism. Oncogene. 2016;35:5989-6000.
38. Liu J, Li X, Yao Y, Li Q, Pan Z, Li Q. miR-1275 controls granulosa cell apoptosis and estradiol synthesis by impairing LRH-1/CYP19A1 axis. Biochim Biophys Acta Gene Regul Mech. 2018;1861:246-257.
39. Cheng Y, Maeda A, Goto Y, Matsuda F, Miyano T, Inoue N, et al. Changes in expression and localization of X-linked inhibitor of apoptosis protein (XIAP) in follicular granulosa cells during atresia in porcine ovaries. J Reprod Dev. 2008;54:454-9.
40. Matsuda F, Inoue N, Goto Y, Maeda A, Cheng Y, Sakamaki K, et al. cFLIP regulates death receptor-mediated apoptosis in an ovarian granulosa cell line by inhibiting procaspase-8 cleavage. J Reprod Dev. 2008;54:314-20.
41. Hatzirodos N, Irving-Rodgers HF, Hummitzsch K, Rodgers RJ. Transcriptome profiling of the theca interna from bovine ovarian follicles during atresia. PLoS One. 2014;9:e99706.
42. Chu YL, Xu YR, Yang WX, Sun Y. The role of FSH and TGF-beta superfamily in follicle atresia. Aging (Albany NY). 2018;10:305-321.
43. Terenina E, Fabre S, Bonnet A, Monniaux D, Robert-Granié C, SanCristobal M, et al. Differentially expressed genes and gene networks involved in pig ovarian follicular atresia. Physiol Genomics. 2017;49:67-80.
44. Wang A, Bao Y, Wu Z, Zhao T, Wang D, Shi J, et al. Long noncoding RNA EGFR-AS1 promotes cell growth and metastasis via affecting HuR mediated mRNA stability of EGFR in renal cancer. Cell Death Dis. 2019;10:154.
45. Salameh A, Lee AK, Cardó-Vila M, Nunes DN, Efstathiou E, Staquicini FI, et al. PRUNE2 is a human prostate cancer suppressor regulated by the intronic long noncoding RNA PCA3. Proc Natl Acad Sci U S A. 2015;112:8403-8.
46. Pan Z, Zhang J, Li Q, Li Y, Shi F, Xie Z, et al. Current advances in epigenetic modification and alteration during mammalian ovarian folliculogenesis. J Genet Genomics. 2012;39:111-23.

47. Yeung CK, Wang G, Yao Y, Liang J, Tenny Chung CY, Chuai M, et al. BRE modulates granulosa cell death to affect ovarian follicle development and atresia in the mouse. Cell Death Dis. 2017;8:e2697.
48. Portela VM, Dirandeh E, Guerrero-Netro HM, Zamberlam G, Barreta MH, Goetten AF et al. The role of fibroblast growth factor-18 in follicular atresia in cattle. Biol Reprod. 2015;92:14.
49. Torres-Ortiz MC, Gutiérrez-Ospina G, Gómez-Chavarín M, Murcia C, Alonso-Morales RA, Perera-Marín G. The presence of VEGF and Notch2 during preantral-antral follicular transition in infantile rats: Anatomical evidence and its implications. Gen Comp Endocrinol. 2017;249:82-92.
50. Liu Z, Hao C, Song D, Zhang N, Bao H, Qu Q. Androgen Receptor Coregulator CTBP1-AS Is Associated With Polycystic Ovary Syndrome in Chinese Women: A Preliminary Study. Reprod Sci. 2015;22:829-37.
51. Li Y, Wang H, Zhou D, Shuang T, Zhao H, Chen B. Up-Regulation of Long Noncoding RNA SRA Promotes Cell Growth, Inhibits Cell Apoptosis, and Induces Secretion of Estradiol and Progesterone in Ovarian Granular Cells of Mice. Med Sci Monit. 2018;24:2384-2390.
52. Wongtrakoongate P, Riddick G, Fucharoen S, Felsenfeld G. Association of the Long Non-coding RNA Steroid Receptor RNA Activator (SRA) with TrxG and PRC2 Complexes. PLoS Genet. 2015;11:e1005615.
53. Huang X, Pan J, Wu B, Teng X. Construction and analysis of a lncRNA (PWRN2)-mediated ceRNA network reveal its potential roles in oocyte nuclear maturation of patients with PCOS. Reprod Biol Endocrinol. 2018;16:73.
54. Carlevaro-Fita J, Johnson R. Global Positioning System: Understanding Long Noncoding RNAs through Subcellular Localization. Mol Cell. 2019;73:869-883.
55. Grelet S, Link LA, Howley B, Obellianne C, Palanisamy V, Gangaraju VK, et al. Addendum: A regulated PNUTS mRNA to lncRNA splice switch mediates EMT and tumour progression. Nat Cell Biol. 2017;19:1443.
56. Peng C, Li L, Zhang MD, Bengtsson Gonzales C, Parisien M, Belfer I, et al. miR-183 cluster scales mechanical pain sensitivity by regulating basal and neuropathic pain genes. Science. 2017;356:1168-1171.
57. Ichiyama K, Dong C. The role of miR-183 cluster in immunity. Cancer Lett. 2019;443:108-114.
58. Gheysarzadeh A, Yazdanparast R. STAT5 reactivation by catechin modulates H_2O_2-induced apoptosis through miR-182/FOXO1 pathway in SK-N-MC cells. Cell Biochem Biophys. 2015;71:649-56.
59. Woldemichael BT, Jawaid A, Kremer EA, Gaur N, Krol J, Marchais A, et al. The microRNA cluster miR-183/96/182 contributes to long-term memory in a protein phosphatase 1-dependent manner. Nat Commun. 2016;7:12594.
60. Muraleedharan CK, McClellan SA, Ekanayaka SA, Francis R, Zmejkoski A, Hazlett LD, et al. The miR-183/96/182 Cluster Regulates Macrophage Functions in Response to Pseudomonas aeruginosa. J Innate Immun. 2019;11:347-358.

61. Mohammed BT, Sontakke SD, Ioannidis J, Duncan WC, Donadeu FX. The Adequate Corpus Luteum: miR-96 Promotes Luteal Cell Survival and Progesterone Production. J Clin Endocrinol Metab. 2017;102:2188-2198.
62. Gebremedhn S, Salilew-Wondim D, Hoelker M, Rings F, Neuhoff C, Tholen E, et al. MicroRNA-183-96-182 Cluster Regulates Bovine Granulosa Cell Proliferation and Cell Cycle Transition by Coordinately Targeting FOXO1. Biol Reprod. 2016;4:27.
63. Myatt SS, Wang J, Monteiro LJ, Christian M, Ho KK, Fusi L, et al. Definition of microRNAs that repress expression of the tumor suppressor gene FOXO1 in endometrial cancer. Cancer Res. 2010;70:367-77.
64. Hou Y, Fu L, Li J, Li J, Zhao Y, Luan Y, et al. Transcriptome Analysis of Potential miRNA Involved in Adipogenic Differentiation of C2C12 Myoblasts. Lipids. 2018;53:375-386.
65. Puri P, Little-Ihrig L, Chandran U, Law NC, Hunzicker-Dunn M, Zeleznik AJ. Protein Kinase A: A Master Kinase of Granulosa Cell Differentiation. Sci Rep. 2016;6:28132.
66. Park Y, Maizels ET, Feiger ZJ, Alam H, Peters CA, Woodruff TK, et al. Induction of cyclin D2 in rat granulosa cells requires FSH-dependent relief from FOXO1 repression coupled with positive signals from Smad. J Biol Chem. 2005;280:9135-48.

Figures

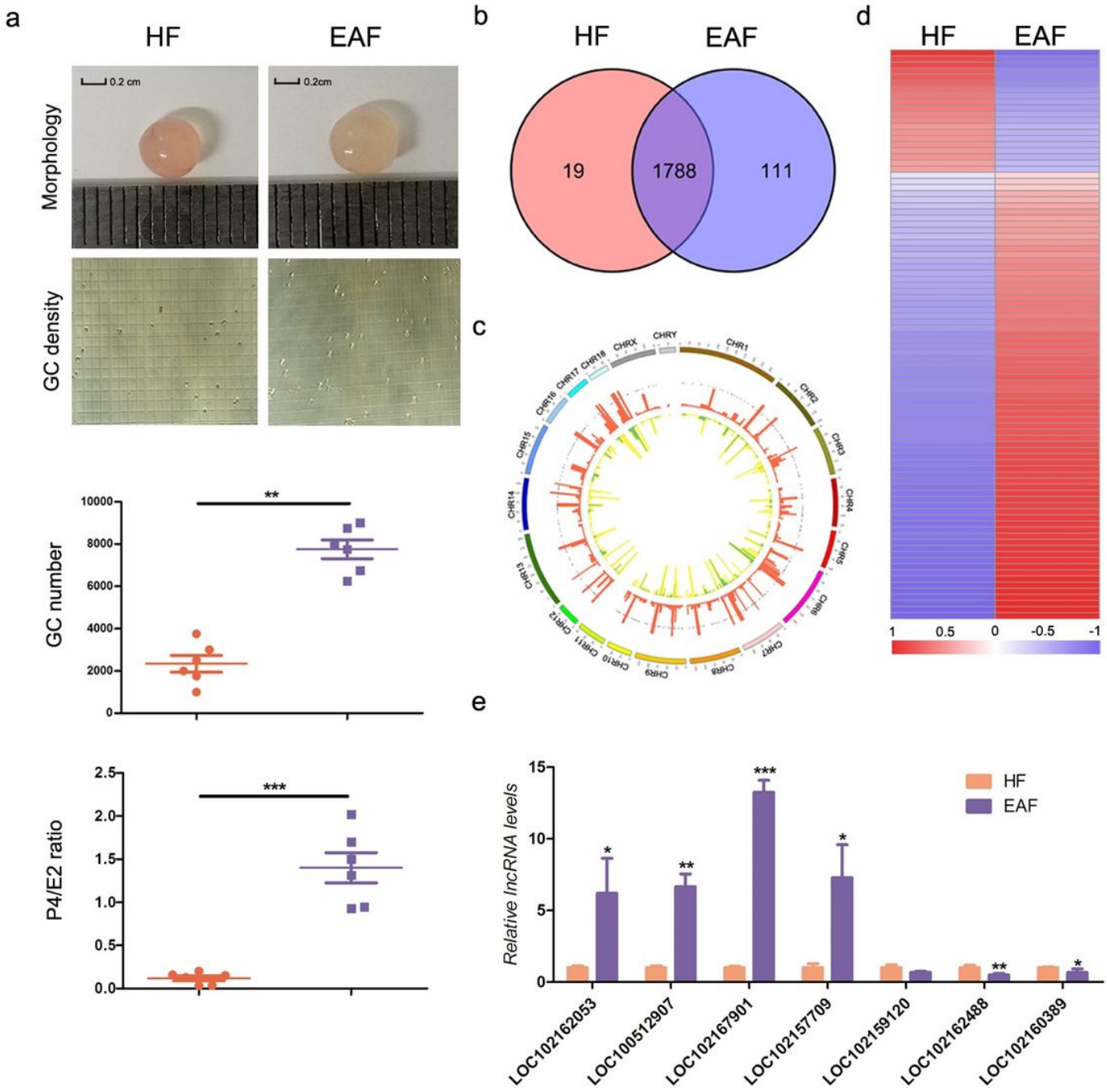

Figure 1

Transcriptome profiles of lncRNAs in porcine ovarian follicles. a Porcine ovarian follicles (3-5 mm diameter) were divided into healthy follicles (HF) and early atresia follicles (EAF) by morphology, granulosa cell (GC) density, ratio of progesterone (P4)/17β-estradiol (E2) concentration in follicular fluid. HF (left panel): (1) the follicles were pink with intensive blood vessels, and clear follicular fluid; (2) the GC density < 4000; (3) the P4/E2 ratio < 1. EAF (right panel): (1) the follicles were pale with turbid follicular fluid, and lack of blood vessels; (2) 4000 ≤ the GC density < 10000; (3) 1 ≤ the P4/E2 ratio < 5. b Venn diagram of the overlap lncRNAs in HF and EAF. c The chromosome distribution and expression schema of lncRNAs. The outermost layer represents chromosomes. The red and yellow histograms represent

lncRNA expression in HF and EAF. d Heatmap for differentially expressed lncRNAs (DELs) between HF and EAF. e Validation of DELs. The expression levels of DELs in HF and EAF were detected by using qRT-PCR. Data are represented as mean ± S.E.M. with at last three independent experiments. * P<0.05. ** P<0.01. *** P<0.001.

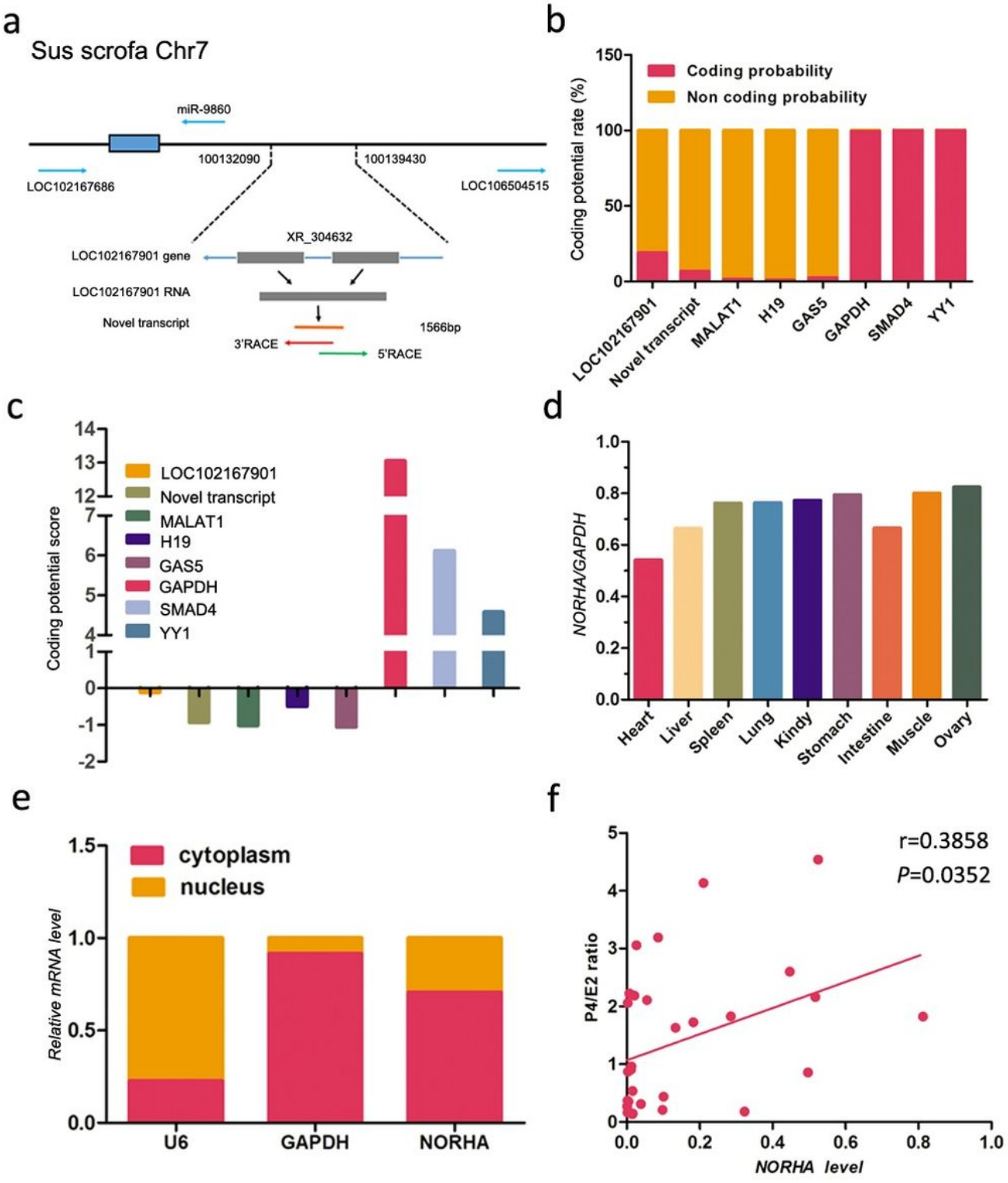

Figure 2

NORHA is a novel cytoplasmic lncRNA involvement of follicular atresia. a Flow diagram showing the strategy for isolation of the full-length of LOC102167901 RNA by RACE assay (Fig.S4a). b, c The coding potential of novel transcript was predicted by CPAT (b) and CPC (c) methods. LOC102167901 is the original sequence from NCBI database. MALAT1, H19 and GAS5 are well known lncRNAs, and GAPDH, SMAD4 and YY1 are protein-coding genes. d Tissue expression profile of NORHA. e Subcellular distribution of NORHA in GCs. Levels of marker genes (GAPDH for cytoplasm and U6 for nuclear) and NORHA in nuclear and cytoplasm were quantified by qRT-PCR. f The correlation of follicular NORHA levels and P4/E2 ratio in follicular fluid.

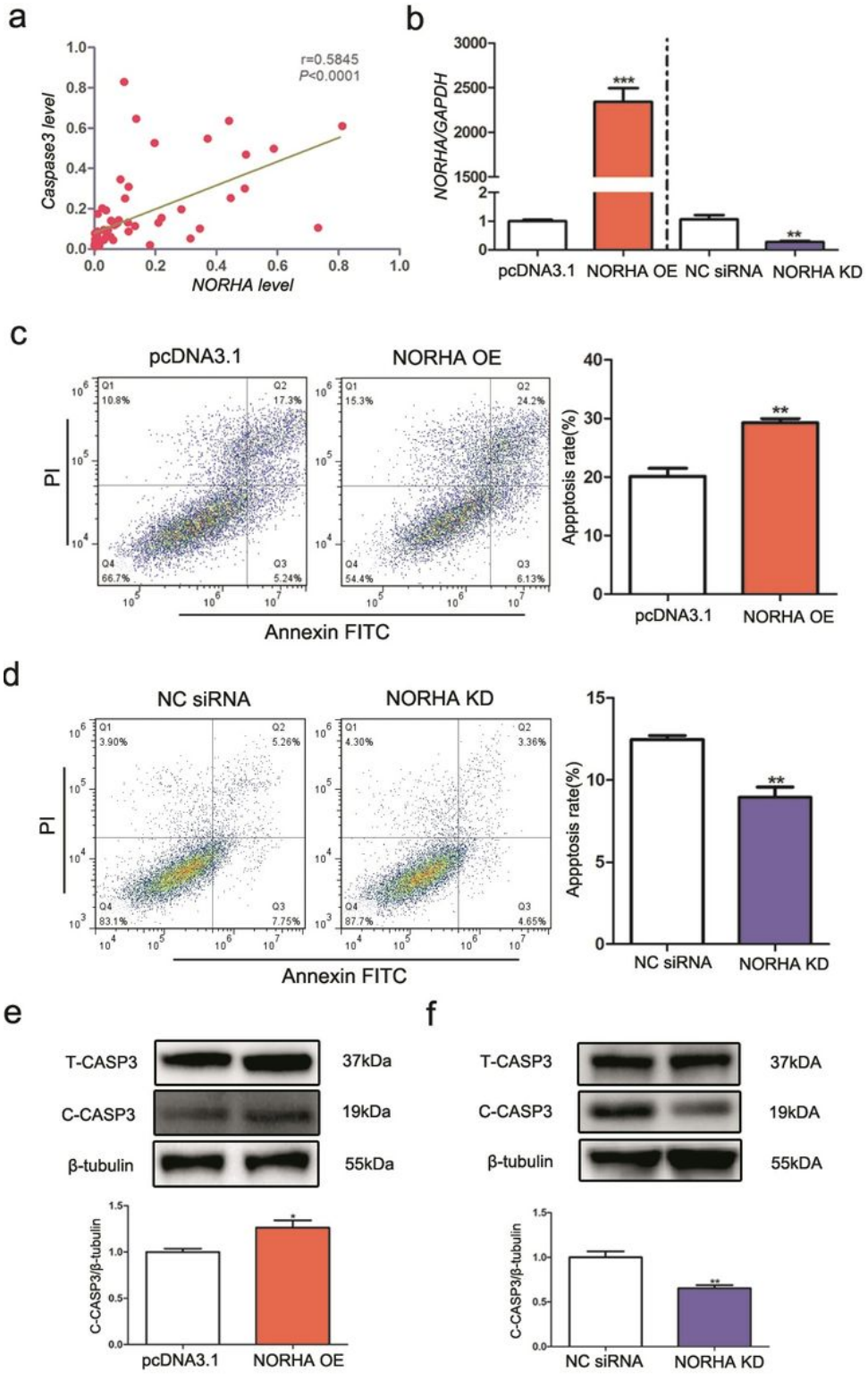

Figure 3

NORHA induces cell apoptosis of the porcine GCs. a Levels of NORHA and Caspase3 mRNA are positively correlated in follicles. b Overexpression and knockdown of NORHA in GCs by transfecting with pcDNA3.1-NORHA or NORHA-siRNA. NORHA levels were detected by RT-PCR and normalized by GAPDH. c, d NORHA controls GC apoptosis. GCs were treated with pcDNA3.1-NORHA (c) and NORHA-siRNA (d), cell apoptosis was detected by flow cytometry. e, f NORHA controls Caspase3 expression in GCs. Cs were treated with

pcDNA3.1-NORHA (e) and NORHA-siRNA (f), and protein levels of total-Caspase-3 (T-CASP3) and cleave-Caspase-3 (C-CASP3) were measured by western blotting. Data are represented as mean ± SEM with at last three independent experiments. * P<0.05. ** P<0.01. *** P<0.001.

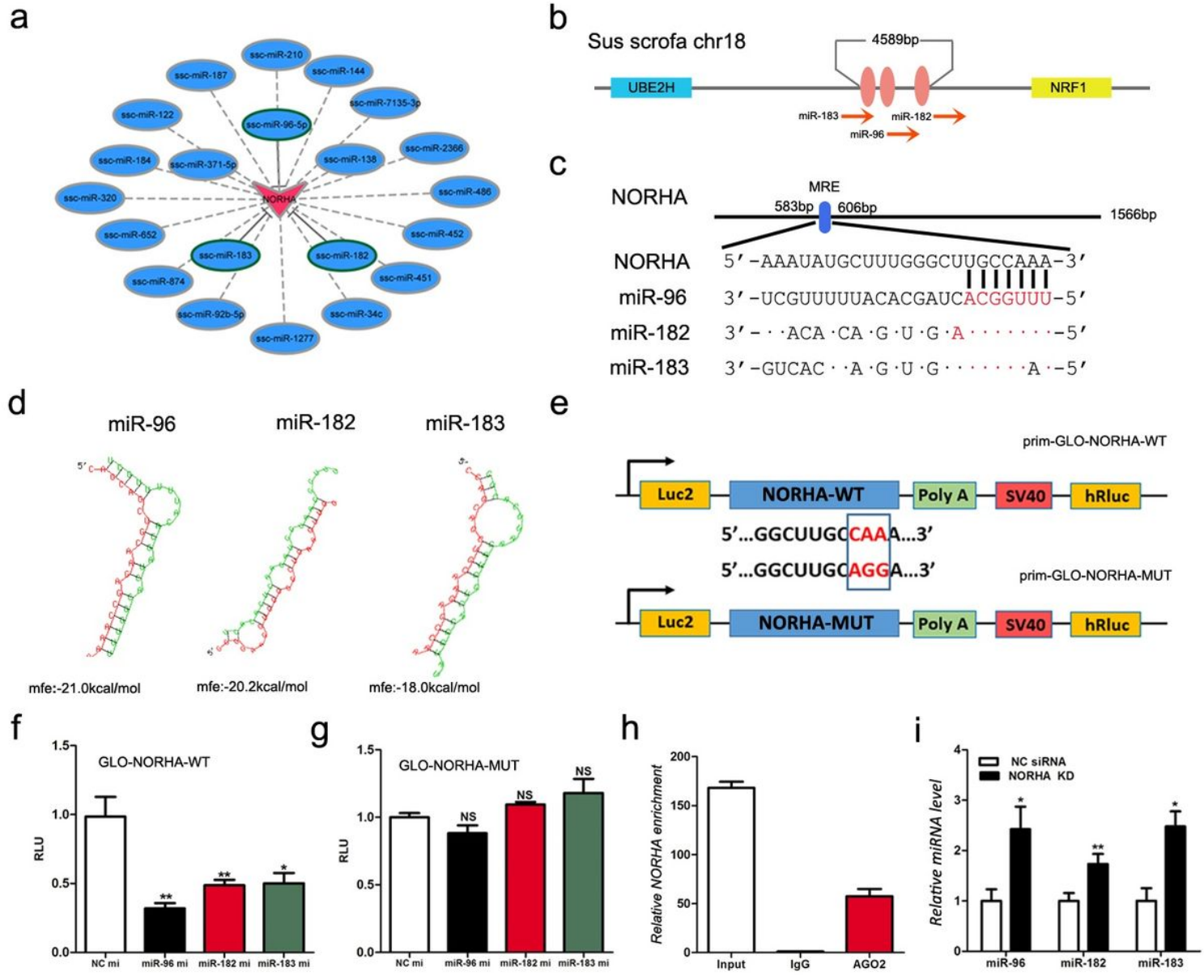

Figure 4

NORHA is a molecular sponge of the miR-183-96-182 cluster. a An interaction network between NORHA and miRNAs that down-regulated in EAF. The data of miRNA-seq were unpublished. The red triangle represents NORHA that was up-regulated in EAF, and blue ellipses represent miRNAs that down-regulated in EAF. b Chromosome location of miR-183, miR-96, and miR-182 show that they are a miRNA cluster from a common genome region. c Schematic showing the interactions of miR-183, miR-96, and miR-182 seed sequences, with NORHA RNA sequence. d Minimum free energy (MFE) of miR-183, miR-96, and miR-182 binding to NORHA were predicted by RNAhybrid. e Schematic showing the reporter constructs of NORHA. NORHA sequence containing wild-typed and mutant-typed miRNA binding site was amplified and inserted into prim-GLO plasmid to construct luciferase report vector. f and g Wild- (f) or mutant-typed (g)

report vector were co-transfected with miR-183 mimics (mi), miR-96 mimics (mi), and miR-182 mimics (mi) into HEK293T cells, luciferase activity was measured. h RIP assay by AGO2-specific antibody. The levels of NORHA enriched on AGO2 protein were detected by qRT-PCR. IgG antibody was used as a negative control. i The levels of miR-183, miR-96 and miR-182 in GCs knockdown of NORHA. Data are represented as mean ± S.E.M. with at last three independent experiments. * P<0.05. ** P<0.01. ns, not significant.

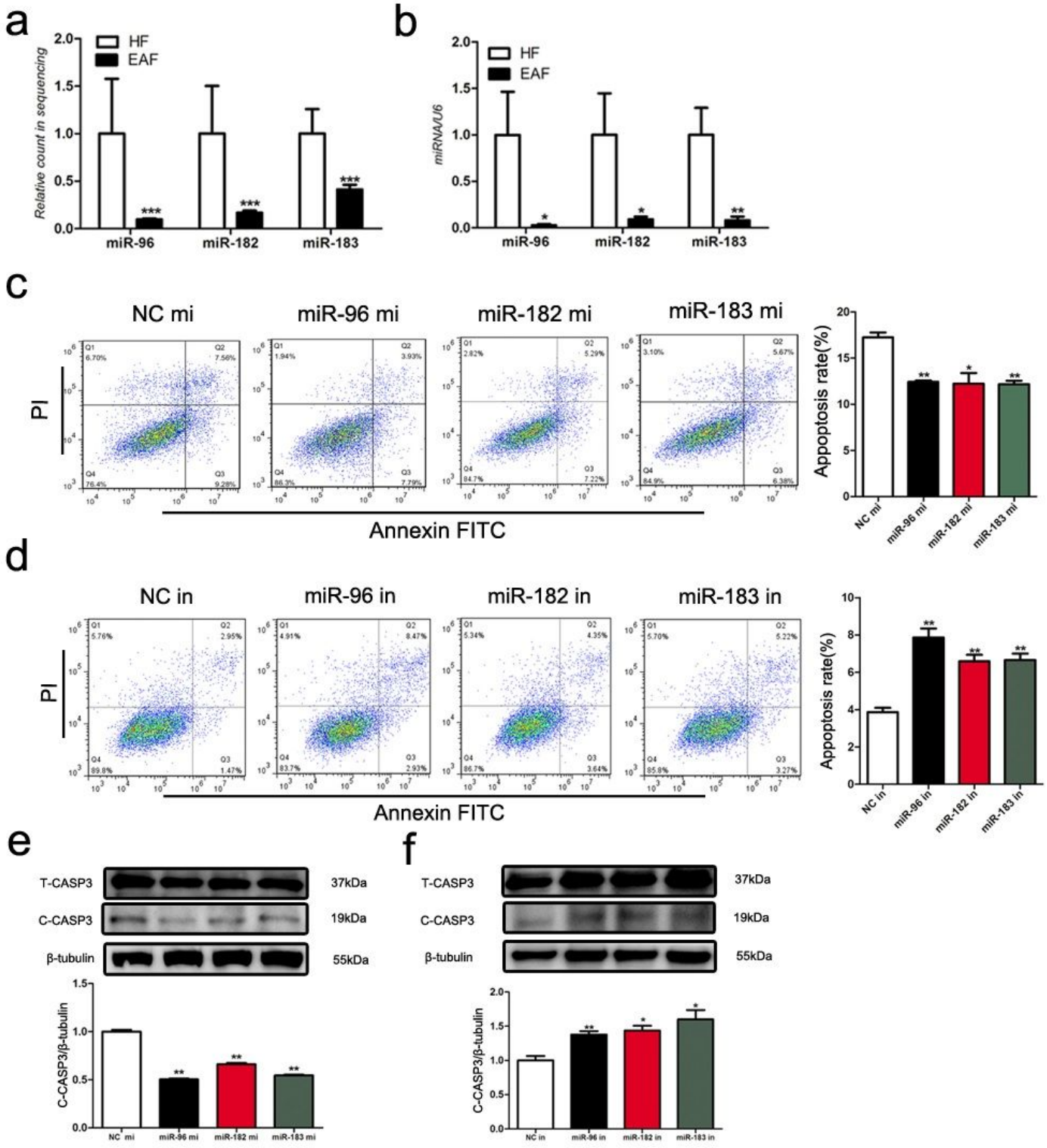

Figure 5

The miR-183-96-182 cluster inhibits GC apoptosis. a and b The expression of the miR-183-96-182 cluster in HF and EAF was detected by RNA-seq (a) and qRT-PCR (b). c, d miR-183-96-182 cluster controls GC apoptosis. GCs were transfected with mimics (mi) (c) or inhibitor (in) (d) of miR-183, miR-96 and miR-182, apoptosis rate was analyzed by flow cytometry. e, f miR-183-96-182 cluster controls Caspase3 expression in GCs. GCs were transfected with mimics (mi) (e) or inhibitor (in) (f) of miR-183, miR-96 and miR-182, and protein levels of T-CASP3 and C-CASP3 were detected by western blot. Data are represented as mean ± S.E.M. with at last three independent experiments. * P<0.05. ** P<0.01. *** P<0.001.

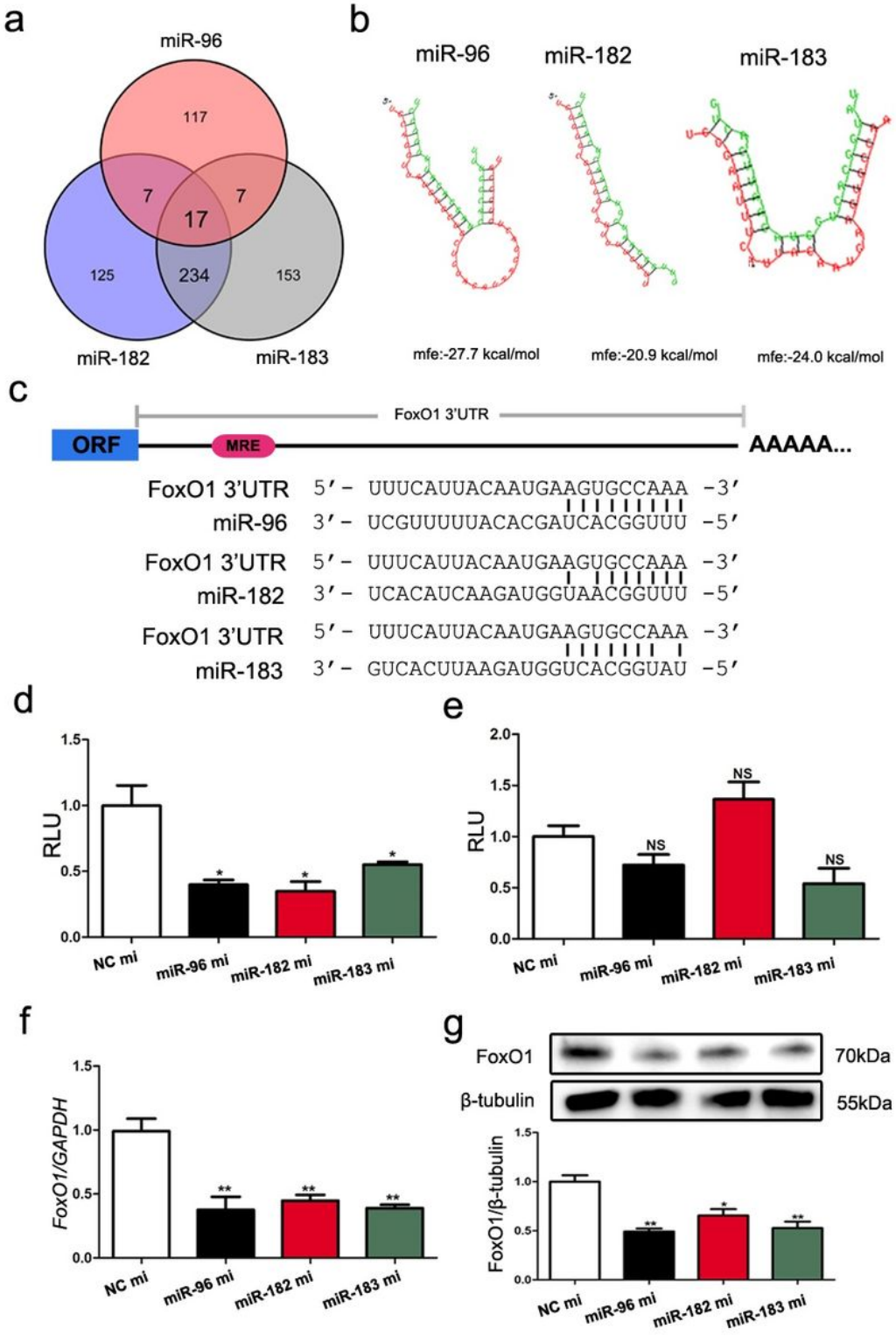

Figure 6

FoxO1 is a common target of the miR-183-96-182 cluster in GCs. a The common putative targets of the miR-183-96-182 cluster. The putative targets of miR-183, miR-96, and miR-182 were predicted by five programs Targetscan, Pictar2, PITA, RNA22, and RNAhybrid. b MFE of the miR-183-96-182 cluster binding to the 3’-UTR of the porcine FoxO1 gene was predicted by RNAhybrid. c The binding sites of the miR-183-96-182 cluster in the 3’-UTR of the porcine FoxO1 gene. d, e Luciferase assay. Luciferase activity was measured in HEK293T cells co-transfected with mimics (mi) of miR-183, miR-96, or miR-182, and reporter vectors of FoxO1 3’-UTR harboring the wild-typed (d) or mutant-typed (e) miRNA binding site, respectively. f and g GCs were transfected with mimics (mi) of miR-182, miR-96, or miR-183, mRNA (f) and protein (g) levels of FoxO1 were detected by qRT-PCR and western blotting. Data are represented as mean ± S.E.M. with at last three independent experiments. * $P<0.05$. ** $P<0.01$. NS, not significant.

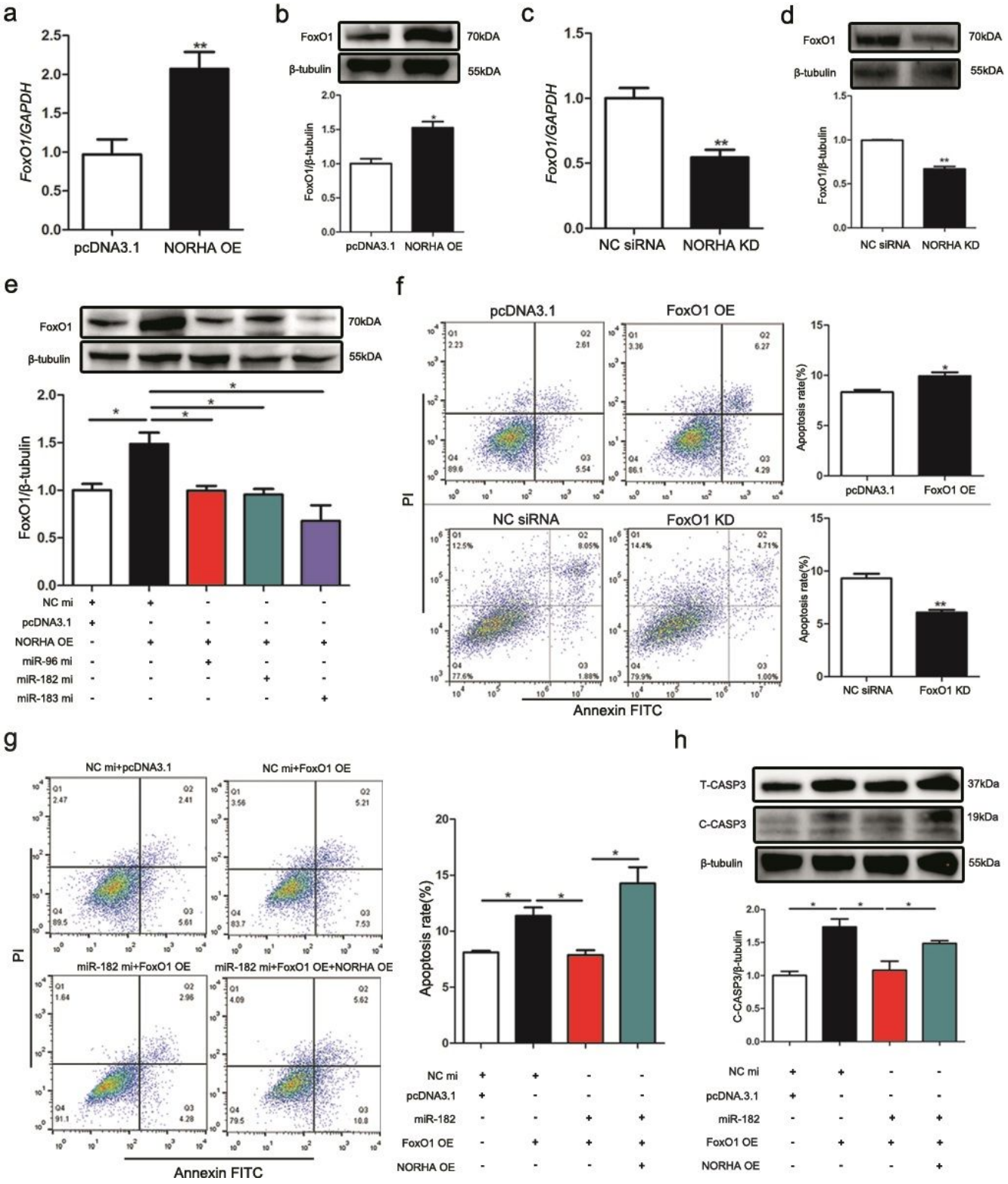

Figure 7

NORHA induces FoxO1-mediated GC apoptosis by competing for miR-183-96-182 cluster. a, d NORHA induces FoxO1 expression. The mRNA (a) and protein (b) levels of FoxO1 were detected in porcine GCs transfected with pcDNA3.1-NORHA. The mRNA (c) and protein (d) levels of FoxO1 were detected in GCs transfected with NORHA-siRNA. e NORHA induces FoxO1 expression via the miR-183-96-182 cluster. GCs were co-transfected with mimics (mi) of miR-183, miR-96, or miR-182, and pcDNA3.1-NORHA, protein

levels of FoxO1 were measured by western blot. f FoxO1 contributes to GC apoptosis. pcDNA3.1-FoxO1 (upper part), or FoxO1-siRNA (lower part) were transfected into GCs, and apoptosis rate was measured by flow cytometry. g, h NORHA induces GC apoptosis via the miR-182/FoxO1 axis. GCs were co-transfected with pcDNA3.1-FoxO1, miR-182 mimics (mi) and pcDNA3.1-NORHA, apoptosis rate (g), and protein levels of T-CASP3 and C-CASP3 (h) were detected. Data are represented as mean ± S.E.M. with at last three independent experiments. * P<0.05. ** P<0.01.

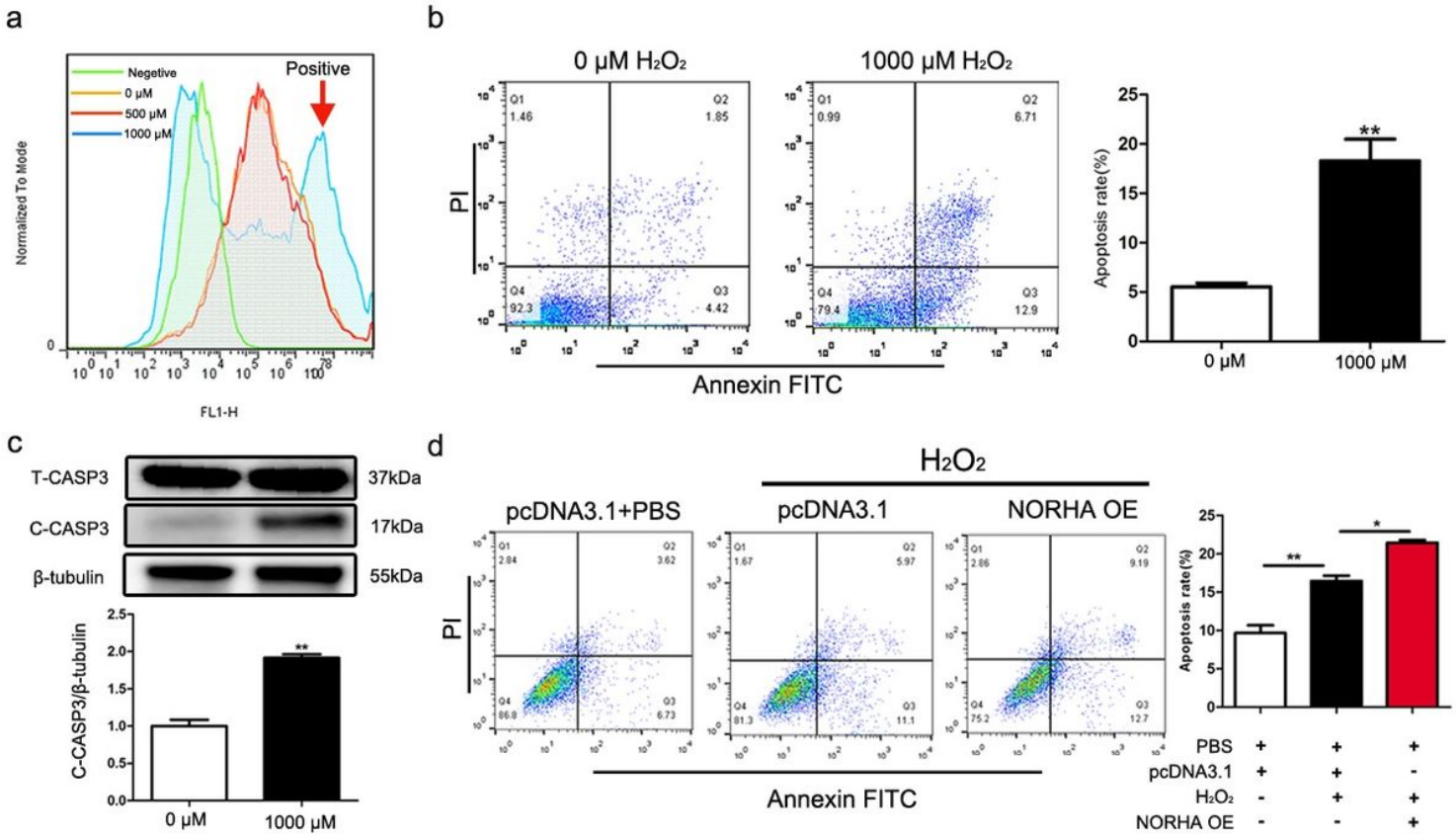

Figure 8

NORHA and oxidative stress synergistically induce GC apoptosis. a H2O2 induces oxidative stress. Porcine GCs were treated with H2O2 (0, 500, and 1000 μM) for 90 min, and reactive oxygen species (ROS) levels were detected by flow cytometry. b, c Oxidative stress induced by H2O2 induces GC apoptosis. The apoptosis rate (b), and protein levels of T-CASP3 and C-CASP3 (c) were measured in GCs with 1000 μM H2O2 treatment. d NORHA and oxidative stress synergistically induced GC apoptosis. GCs were treated with pcDNA3.1-NORHA with or without H2O2 treatment, and the apoptosis rate was calculated. Data are represented as mean ± S.E.M. with at last three independent experiments. * P<0.05. ** P<0.01.

Supplementary Files

This is a list of supplementary files associated with this preprint. Click to download.

- SupplementalFigure.doc

- SupplementalTable.docx